

University of Rhode Island

DigitalCommons@URI

Computer Science and Statistics Faculty
Publications

Computer Science and Statistics

2-2020

Effect of Radiation Dose Fractionation and Radiation Energy on Gold Nanoparticle Enhancement of Radiation Therapy

Bindeshwar Sah

Jing Wu

Adam Vanasse

Michael Antosh

Follow this and additional works at: https://digitalcommons.uri.edu/cs_facpubs



Effect of radiation dose fractionation and radiation energy on gold nanoparticle enhancement of radiation therapy

Bindeshwar Sah¹; Jing Wu²; Adam Vanasse¹; Michael P Antosh^{1,3,*}

¹Department of Physics, University of Rhode Island. 2 Lippitt Rd, Kingston RI 02881.

²Department of Computer Science and Statistics, University of Rhode Island. 9 Greenhouse Rd, Kingston RI 02881.

³Institute for Brain and Neural Systems, Brown University. 184 Hope St, Providence RI 02912.

***Corresponding Author(s): Michael P Antosh**

Department of Physics, University of Rhode Island, 2
Lippitt Road, Kingston, RI, 02881
Email: mantosh@uri.edu

Abstract

Objective: Gold nanoparticles (GNPs) have the potential to enhance the effects of radiation therapy, using Auger electrons to cause additional damage to tumors. In this work, we explore the effect of two clinically important variables: dose fractionation and radiation energy. In clinical radiation therapy, radiation is fractionated (split into multiple sessions) and high-energy radiation is used. However, in the field of GNP research, radiation has generally been given in one session and lower radiation energies have generally been used.

Methods: Mice with JC breast tumors implanted in the flank were given radiation therapy over 1, 2, or 4 fractions, with radiation energies of either 250 kilovolts peak or 350 kilovolts peak. A survival analysis and a weighted generalized estimating equation analysis were used to.

Results: The use of multiple radiation fractions (between 1 and 4) and the use of radiation doses between 250-350 kVp were only different by statistically insignificant amounts, after the contributions from time, sex, age at irradiation and original tumor volume were accounted for. A survival analysis found a higher likelihood of death for female mice, mice given 350 kilovolts peak radiation (versus 250 kilovolts peak), and mice with larger tumors, as well as a lower likelihood of death for mice irradiated at an older age; fractionated radiation did not have a statistically significant effect.

Conclusion: These results suggest that GNPs have the potential to enhance radiation therapy when used with fractionated radiation.

Received: Dec 16, 2019

Accepted: Feb 03, 2020

Published Online: Feb 06, 2020

Journal: Journal of Nanomedicine

Publisher: MedDocs Publishers LLC

Online edition: <http://meddocsonline.org/>

Copyright: © Antosh MP (2020). *This Article is distributed under the terms of Creative Commons Attribution 4.0 International License*



Introduction

Gold nanoparticles (GNPs) have been shown to have the potential to enhance radiation therapy [1-22]. Gold absorbs significantly better than human tissue [23], and after an interaction with radiation gold releases extra electrons via the Auger effect. Depending on the situation, there could be the potential for approximately 10 extra electrons per interaction, although some electrons may interact inside of the nanoparticles themselves [24].

Although GNPs have been shown to have potential, gold has not yet translated to clinical use. In this work, we examine the effect *in vivo* of an important clinical variable: radiation dose fractionation. In clinical radiation therapy, it is very common for treatments to be done in fractions (multiple sessions), which allow healthy tissue time to heal during the treatments [25]. Yet, of all of the animal experiments done with GNPs and radiation therapy, to the authors' knowledge only one experiment has used fractionated radiation with GNPs, and this experiment did not compare fractionated radiation treatments with a treatment involving only one radiation treatment [19]. This may be because GNPs can leave the body quickly – for example, in a pioneering work Hainfeld et al. [9] gave (one fraction of) radiation therapy only minutes after the injection of gold. In previous work in the authors' laboratory [16], we found that an appreciable amount of gold stayed in mouse tumors for at least one week (after intratumoral injection) when conjugated to the cancer-targeting molecule pH-Low Insertion Peptide [26]. This period of time is fairly close to the total time period used for fractionated radiation therapy in human cancer in the CHART study (continuous hyperfractionated accelerated radiation treatment), which gave 36 radiation fractions over 12 days [25,27].

As a secondary result, we looked at the effect of radiation energy. With the exception of the jumps at shell energies (K-shell, L-shell, M-shell for the photoelectric effect), the absorption of radiation by gold (mass attenuation coefficient) decreases with increasing photon energy until approximately 4 MeV, then increases by roughly 50% by 20 MeV. In particular, the mass attenuation coefficient decreases by a factor of approximately 105 between 100 keV (a representative imaging energy) and 10 MeV (a representative treatment energy) (data from the National Institute of Standards and Technology [28], inspired by figure in Hainfeld et al. [23]). Despite this, several papers have shown that GNPs can still be effective at MeV-scale radiation energies (for example, [6,7,12,15,17]) In this paper, we compare two energies: 250 and 350 kVp (kilovolts peak).

The overall goal of this paper is to contribute to the ongoing investigation into the clinical relevance of GNPs. The results shown below shed further light onto the effect of dose fractionation and radiation energy.

Methods

Overall Outline of Work

The overall outline of the experimental work can be summarized as:

- Inject mice with cells
- Inject mice with gold nanoparticle treatment
- Irradiate: over 1, 2 or 4 fractions (24 hours apart); radiation energy either 250 kVp or 350 kVp

- Measure tumor size as a function of time

Gold nanoparticle preparation

Monomaleido 1.9 nm gold nanoparticles were purchased from Nanoprobes, Inc. (stock number 2010). Gold nanoparticles were conjugated to pH-Low Insertion Peptide using the same methodology as Sah et al [16].

Mouse experiment

Mouse experimental protocols were approved by the Institutional Animal Care and Use Committee (IACUC) at the University of Rhode Island. The 43 Balb/C mice tracked for tumor size in this experiment were purchased from Envigo. At approximately 5-15 weeks of age, mice were injected in the right flank (after hair removal with cream) with approximately 1.5 million JC (mouse breast cancer, from ATCC) cells in a 100 μ L mixture with Roswell Park Memorial Institute (RPMI) medium. When mouse tumors reached approximately 5-8 mm in length (similar to Yao et al. [29]), mice were injected intratumorally with approximately 200 μ g of GNPs (similar to Sah et al. [16]), conjugated to pH-Low Insertion Peptide, in a 50 μ L mixture with phosphate buffer solution. Age of mice at irradiation is included in supplementary table S1.

Some mice were injected with tumors, but the tumors did not grow; these mice were excluded from the rest of the experiment. The authors excluded age at injection from the statistical analyses to avoid multicollinearity because age at injection was strongly correlated with age at irradiation.

4 hours after injection (similar to Sah et al. [16]), mice were irradiated in a cabinet x-ray machine (Faxitron MultiRad 350; dose measured using an ionization chamber from Radcal). A total dose of 20 gray of radiation was given to mice, over 1, 2 or 4 dose fractions. Mice given 2 dose fractions were given 10 gray per fraction on consecutive days; mice given 4 dose fractions were given 5 gray per fraction on each of 4 consecutive days. Due to an issue with number of mice, no female mice were given 4 radiation fractions. Mice were irradiated with lead covering all but an approximate semi-circle of diameter 1 inch around the tumor (dose similar to Sah et al. [16]); shape similar to Hainfeld et al. [9]). Maximum voltage of the machine was set to either 250 kiloVolts peak (250 kVp (keV peak) radiation energy spectrum) or 350 kiloVolts (350 kVp). A Thoraeus-1 filter was used on the radiation. Supplementary table S1 shows the number of mice in each experimental group: 7 males and 7 females in 250 kVp/1fraction. 3 males and 6 females in 250 kVp/2 fractions, 6 males and 0 females in 250 kVp/4 fractions, 7 males and 7 females in 350 kVp/1 fraction.

Mouse tumor size was tracked for approximately one month after irradiation. Any data recorded in days 1-28 was included in the analysis and plots (days 29-30 may not have been recorded, for example, if days 29 and 30 were a weekend; some but not all mice were recorded for a few days past 30). Mice were euthanized, using carbon dioxide, if mice reached the end time point, if mice reached the maximum tumor size (20 mm, one mouse), if mice had necrotic skin (one mouse) or if mice were sick (one mouse, which was hunched). 14 of the 43 mice were found dead. Supplementary table S1 shows each mouse, the treatment it was given, and the reason for euthanasia (or if it was found dead). Tumor volume was calculated using the formula $\text{volume} = (1/2) \cdot (\text{length}) \cdot (\text{width})^2$, where length is larger than width [30].

Mice were anesthetized using isoflurane gas anesthesia during 3 types of procedures: Hair removal/cell injection, nanoparticle injection and irradiation.

Two mice were injected intravenously with GNPs, instead of intratumorally (intentionally). Due to the small sample size, these mice were not included in the plots or analysis.

Analysis

We considered the longitudinal tumor size measurements of 45 mice between day 0 to day 28. Some mice were euthanized during the study when tumors reached a large size (approx. 20 mm length) or when skin became necrotic. The reasons of dropout were thus known (listed in supplementary table S1) and were also included in the analysis as covariates, which makes the missing data mechanism most likely missing at random (MAR). Thus, an observation-specific weighted generalized estimating equation (WGEE) [31] was adopted to analyze the tumor size data, where each measure was weighted by the inverse probability of being observed using a logistic regression model. Furthermore, the identity link function was assumed, and the compound symmetric working correlation structure was selected using the deviance information criterion (DIC) [32] based on the completely observed data. Covariates considered in the WGEE approach include day number after irradiation, age of mouse at irradiation, tumor volume at irradiation, sex (male or female), radiation energy and radiation fractions. All the continuous covariates were standardized. Comparisons of treatment groups in terms of radiation fractions (1, 2, and 4) were done, with corrections for multiple hypothesis testing using a Tukey-Kramer adjustment.

Cox regression analysis [33] was further performed to evaluate whether the occurrence of early death of mice was associated with certain covariates, including age of mouse at irradiation, tumor volume at irradiation, sex, radiation energy, and radiation fractions. Hazard ratios and associated p values were reported for each covariate.

Results

WGEE- The model for longitudinal response

Results of the tumor size measurements are shown in figure 1, and the analysis of these measurements is shown in tables 1 and 2. The results of the analysis show that log (time), log(time) squared, age at irradiation and tumor volume at irradiation are statistically significant. The dependence on log(time) and $(\log(\text{time}))^2$ suggests that the tumors have exponential behavior with time. Tumor volume at the time of irradiation is significant, indicating that a larger original tumor volume leads to larger tumor volumes at later time points compared to tumors that started at a smaller volume. An effect on tumor size from age at irradiation may be related to the fact that radiation can affect organisms of different ages in different ways – for examples, see Hall and Giaccia [25].

Table 1. Results of longitudinal analysis. The logarithm of time, the square of logarithm of time, age at irradiation, tumor volume at irradiation and sex are found to have a statistically significant effect on tumor volume as a function of time. The effect of energy was found to be statistically insignificant. The number of radiation fractions is best evaluated by comparing all of the values to each other, which is done in table 2.

Table 1: Results of longitudinal analysis.

Parameter Estimates for Response Model with Empirical Standard Error Estimates						
Parameter		Estimate	Standard Error	95% Confidence Limits	Z Score	P Value (Prob. > Z)
Intercept		-0.3579	0.1669	(-0.6850, -0.0307)	-2.14	0.0321
Log(time)		-0.5313	0.0797	(-0.6874, -0.3751)	-6.67	<0.0001
(Log(time)) ²		0.2201	0.0292	(0.1630, 0.2773)	7.55	<0.0001
Age at Irradiation		-0.2378	0.0599	(-0.3552, -0.1204)	-3.97	<0.0001
Tumor Volume at Irradiation		0.1506	0.0629	(0.0274, 0.2738)	2.40	0.0166
Sex	Female, compared to Male	0.5093	0.1780	(0.1604, 0.8581)	2.86	0.0042
Energy	350 kVp, compared to 250 kVp	-0.0291	0.1586	(-0.3401, 0.2818)	-0.18	0.8543
Number of Radiation Fractions	2, compared to 1	0.5000	0.2413	(0.0270, 0.9730)	2.07	0.0383
Number of Radiation Fractions	4, compared to 1	0.3350	0.1838	(-0.0252, 0.6953)	1.82	0.0683

As shown in table 2, the different values for radiation fraction (1, 2, and 4 fractions) are not different from each other by a statistically significant fraction. This result is interesting, because it takes place in a model where other statistically signifi-

cant variables are accounted for. This suggests that GNPs can be similarly effective with fractionated radiation, and at different radiation energies.

Table 2: Comparison of means for radiation fractionation. P values were adjusted for multiple hypothesis testing using the Tukey-Kramer method [34].

Differences of Least Squares Means						
Treatment 1	Treatment 2	Estimate (Treatment 1 – Treatment 2)	Standard Error	z Value	P Value (Prob. > z)	Adjusted P Value
2 Radiation Fractions	4 Radiation Fractions	0.1649	0.2321	0.71	0.4774	0.7572
2 Radiation Fractions	1 Radiation Fraction	0.5000	0.2413	2.07	0.0383	0.0958
4 Radiation Fractions	1 Radiation Fraction	0.3350	0.1838	1.82	0.0683	0.1621

WGEE-The model for missingness

To reduce the bias caused by missing data (i.e. the mice no longer being in the data set after being euthanized or found dead), each longitudinal tumor size measure was weighted by the inverse probability of being observed using a logistic regression model. The results of this analysis are shown in table 3. Female mice were found to be more likely to be missing (represented by a negative estimate). In addition, mice irradiated at

an older age and mice given two radiation fractions were less likely to be missing (two radiation fractions compared to mice given one radiation fraction). The added risk to female mice may be because this experiment uses breast cancer. With the radiation fractions, it's possible that the use of two radiation fractions allows healthy tissue more ability to recover (similar to chapter 23 in [25]).

Table 3: Missingness model (reasons for mice with missing data points). A negative value for estimate means more likely to be missing. Results show that mice with larger tumor volumes and female mice were less likely to be seen in the model. Mice given 2 radiation dose fractions were more likely to be seen than mice given only one radiation dose fraction.

Parameter Estimates for Missingness Model						
Parameter		Estimate	Standard Error	95% Confidence Limits	Z Score	P Value (Prob. > Z)
Intercept		8.8814	3.5392	(1.9447,15.8181)	2.51	0.0121
Log(time)		-3.2227	2.9422	(-8.9893,2.5440)	-1.10	0.2734
(Log(time)) ²		0.4946	0.6093	(-0.6997,1.6888)	0.81	0.4170
Y_{t-1}		-0.2793	0.1347	(-0.5434,-0.0152)	-2.07	0.0382
Age at Irradiation		0.9680	0.4589	(0.0685,1.8674)	2.11	0.0349
Tumor Volume at Irradiation		-0.1361	0.2433	(-0.6129,0.3407)	-0.56	0.5759
Sex	Female, compared to Male	-1.1771	0.5011	(-2.1592,-0.1950)	-2.35	0.0188
Energy	350 kVp, compared to 250 kVp	-0.0444	0.5298	(-1.0829,0.9940)	-0.08	0.9331
Number of Radiation Fractions	2, compared to 1	2.6522	1.0515	(0.5913,4.7132)	2.52	0.0117
Number of Radiation Fractions	4, compared to 1	0.9333	1.1167	(-1.2554,3.1221)	0.84	0.4033

Survival model

As mentioned in the methods section and supplementary table S1, several mice were found dead at various points in the experiment. To examine the effect of experimental variables on this effect, a survival analysis was run. The results of this analysis, shown in table 4, found that mice with larger initial tumor volumes, female mice, and mice given 350 kVp radiation had

higher risk of early deaths. The age of mice at irradiation was found to have a reverse effect – younger mice (at time of irradiation) were associated with a significantly increased risk of early deaths. The use of 2 or 4 radiation fractions resulted in a statistically insignificant effect.

Table 4: Survival analysis results. Negative values for estimate mean that survival was more likely; positive values for estimate mean that survival was less likely. Statistically significant variables with less likely survival included larger tumors (at time of irradiation), female mice and mice given 350 kVp radiation. Older mice (at time of irradiation) were more likely to survive. Chi-square is equal to (estimate/standard error)²; hazard ratio = exp (estimate).

Parameter		Degrees of Freedom	Estimate	Standard Error	Chi-Square	P Value	Hazard Ratio
Age at Irradiation		1	-3.43806	0.82965	17.1728	<0.0001	0.032
Tumor Volume at Irradiation		1	0.76861	0.31463	5.9679	0.0146	2.157
Sex	Female, vs. Male	1	2.70689	0.68295	15.7096	<0.0001	14.983
Energy	350 kVp, vs. 250 kVp	1	1.86470	0.62243	8.9751	0.0027	6.454
Radiation Fractions	2, vs. 1	1	-1.45585	0.84453	2.9717	0.0847	0.233
Radiation Fractions	4, vs. 1	1	-1.65536	1.70830	0.9390	0.3325	0.191

Conclusion

The longitudinal analysis of tumor size results described in this paper (tables 1 and 2) indicate that 1, 2 and 4 fractions of radiation were differently only by a statistically insignificant amount after other covariates such as sex, tumor volume at irradiation and age at irradiation were accounted for. The missingness model (table 3) found that female mice were less likely to survive, and mice were more likely to survive if irradiated at an older age or given two radiation fractions (compared to one radiation fraction). In a survival analysis (table 4), higher radiation energy (350 kVp), female mice, mice with larger initial tumors, and mice irradiated at an early age had higher risk of early deaths.

Overall, these results suggest that GNPs could be useful in fractionated radiation done over multiple days, since the tumor size is not significantly changed and the missingness model indicates that the mice are actually somewhat more likely to survive. This is consistent as well with the gold uptake results in Sah et al. [16]), which show that GNPs (targeted using pH-Low Insertion Peptide) can be made to stay in a mouse for at least one week.

With radiation energy, 250 and 350 kVp treatment energies produced similar tumor volumes, although 350 kVp resulted in reduced survival. Previous research suggests that GNPs can be useful at higher radiation energies (for example, [6,7,12,15,17]).

Since the one existing paper using fractionated radiation and GNPs (Geng et al. [19]) did not compare fractionated radiation with non-fractionated radiation, a comparison between the two papers' results cannot be done. However, it is promising that Geng et al. found that fractionated radiation plus GNPs (conjugated to polyethylene glycol and glucose) reduced tumor size compared to fractionated radiation alone. The "250 kVp, 1 fraction" group in this experiment (figure 1) followed the same methodology as the "Targeted Gold + Rad" treatment in previous work by our research group [16]. The mice in the previous work saw tumor volume decrease by a factor of approximately 2-3 over one month; here, the tumor volumes increased by approximately 60-70% by the end of one month. In the female mice, the average tumor size (a significant variable in table 1) was larger in this experiment; in the male mice, the tumor volume was reduced at approximately 15 days but then increased, perhaps suggesting an age-related effect; the age at injection was significantly more varied overall in the previous work.

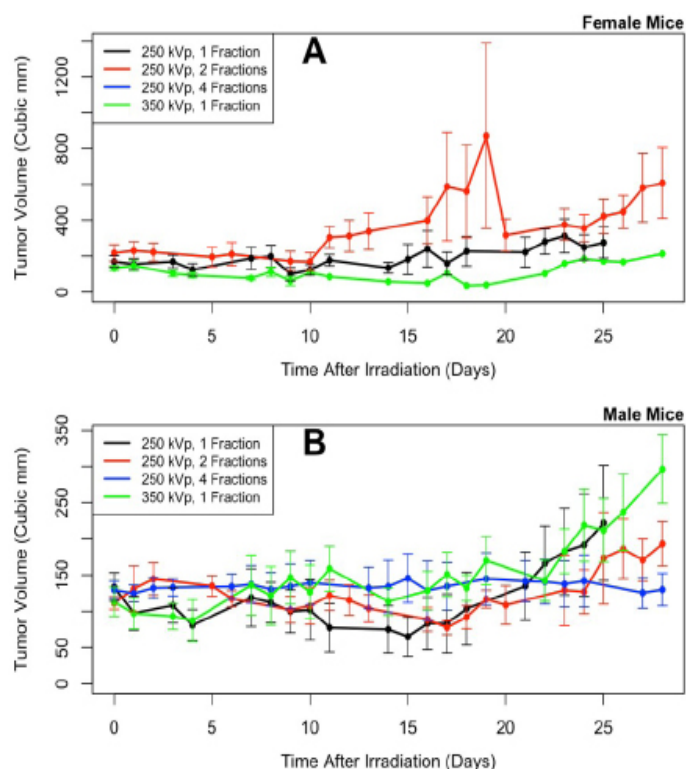


Figure 1: Tumor volume as a function of time after irradiation, in female (A) and male (B) mice.

Mean and standard error of the mean are plotted; any plot with no error bars is a data point from only one mouse. Analysis shows that the number of fractions and the radiation energy have no statistically significant effect once other important variables such as initial tumor volume and age at irradiation are accounted for.

Future research could definitely improve on these results. It would be useful to compare the results to a matching fractionated radiation treatment that does not use GNPs, and perhaps a different size of GNP could be found to produce stronger reductions in tumor size. More fractions (and smaller doses per fraction) would be useful, as would testing a wider array of radiation energies, using intravenous injections and having female mice for every fractionation level.

This research suggests that GNPs may be able to achieve clinical relevance. Hopefully future work will advance this position further, and hopefully GNPs will someday be clinically useful.

Acknowledgements

Research reported in this paper was supported by the In-

stitutional Development Award (IDeA) Network for Biomedical Research Excellence from the National Institute of General Medical Sciences of the National Institutes of Health under grant number P20GM103430. M.A. and J.W. would also like to acknowledge startup funding from the University of Rhode Island.

References

- Libutti SK, Paciotti GF, Byrnes AA, Alexander HR Jr, Gannon WE, et al. Phase I and pharmacokinetic studies of CYT-6091, a novel PEGylated colloidal gold-rhTNF nanomedicine. *Clin Cancer Res.* 2010; 16: 6139-6149.
- Bobyk L, Edouard M, Deman P, Vautrin M, Pernet-Gallay K, et al. Photoactivation of gold nanoparticles for glioma treatment. *Nanomedicine.* 2013; 9: 1089-1097.
- Chang MY, Shiau AL, Chen YH, Chang CJ, Chen HH, et al. Increased apoptotic potential and dose-enhancing effect of gold nanoparticles in combination with single-dose clinical electron beams on tumor-bearing mice. *Cancer Sci.* 2008; 99: 1479-1484.
- Chattopadhyay N, Cai Z, Kwon YL, Lechtman E, Pignol JP, Reilly RM, et al. Molecularly targeted gold nanoparticles enhance the radiation response of breast cancer cells and tumor xenografts to X-radiation. *Breast Cancer Res Treat.* 2013; 137: 81-91.
- Tu Y, Yang W, Bao Y, Chen N, et al. BSA capped Au nanoparticle as an efficient sensitizer for glioblastoma tumor radiation therapy. *RSC Advances.* 2015; 5: 40514-40520.
- Davidi ES, Dreifuss T, Motiei M, Shai E, Bragilovski D, Lubimov L et al. Cisplatin-conjugated gold nanoparticles as a theranostic agent for head and neck cancer. *Head Neck.* 2018; 40: 70-78.
- Dou Y, Guo Y, Li X, Li X, Wang S, et al. Size-Tuning Ionization To Optimize Gold Nanoparticles for Simultaneous Enhanced CT Imaging and Radiotherapy. *ACS Nano.* 2016; 10: 2536-2548.
- Hainfeld JF, Dilmanian FA, Zhong Z, Slatkin DN, Kalef-Ezra JA, et al. Gold nanoparticles enhance the radiation therapy of a murine squamous cell carcinoma. *Phys Med Biol.* 2010; 55: 3045-3059.
- Hainfeld JF, Slatkin DN, & Smilowitz HM. The use of gold nanoparticles to enhance radiotherapy in mice. *Phys Med Biol.* 2004; 49: 309-315.
- Hainfeld JF, Smilowitz HM, O'Connor MJ, Dilmanian FA, Slatkin DN. Gold nanoparticle imaging and radiotherapy of brain tumors in mice. *Nanomedicine (Lond).* 2013; 8: 1601-1609.
- Joh DY, Sun L, Stangl M, Al Zaki A, Murty S, et al. Selective targeting of brain tumors with gold nanoparticle-induced radiosensitization. *PLoS One.* 2013; 8: e62425.
- Kefayat A, Ghahremani F, Motaghi H, Mehrgardi MA. Investigation of different targeting decorations effect on the radiosensitizing efficacy of albumin-stabilized gold nanoparticles for breast cancer radiation therapy. *Eur J Pharm Sci.* 2019; 130: 225-233.
- Kim JK, Seo SJ, Kim HT, Kim KH, Chung MH, et al. Enhanced proton treatment in mouse tumors through proton irradiated nanoradiator effects on metallic nanoparticles. *Phys Med Biol.* 2012; 57: 8309-8323.
- Komatsu T, Nakamura K, Okumura Y, Konishi K. Optimal method of gold nanoparticle administration in melanoma-bearing mice. *Exp Ther Med.* 2018; 15: 2994-2999.
- Popovtzer A, Mizrachi A, Motiei M, Bragilovski D, Lubimov L, et al. Actively targeted gold nanoparticles as novel radiosensitizer agents: an in vivo head and neck cancer model. *Nanoscale.* 2016; 8: 2678-2685.
- Sah B, Shrestha S, Wu J, Vanasse A, Cooper LN, et al. Gold Nanoparticles Enhance Radiation Therapy at Low Concentrations, and Remain in Tumors for Days. *Journal of biomedical nanotechnology.* 2019; 15: 1960-1967.
- Zhang XD, Chen J, Luo Z, Wu D, Shen X, et al. Enhanced tumor accumulation of sub-2 nm gold nanoclusters for cancer radiation therapy. *Adv Healthc Mater.* 2014; 3: 133-141.
- Zhang XD, Wu D, Shen X, Chen J, Sun YM, et al. Size-dependent radiosensitization of PEG-coated gold nanoparticles for cancer radiation therapy. *Biomaterials.* 2012; 33: 6408-6419.
- Geng F, Xing JZ, Chen J, Yang R, Hao Y, et al. Pegylated glucose gold nanoparticles for improved in-vivo bio-distribution and enhanced radiotherapy on cervical cancer. *J Biomed Nanotechnol.* 2014; 10: 1205-1216.
- Yang C, Bromma K, Sung W, Schuemann J, Chithrani D. Determining the Radiation Enhancement Effects of Gold Nanoparticles in Cells in a Combined Treatment with Cisplatin and Radiation at Therapeutic Megavoltage Energies. *Cancers (Basel).* 2018; 10.
- Elahi N, Kamali M, Baghersad MH. Recent biomedical applications of gold nanoparticles: A review. *Talanta.* 2018; 184: 537-556.
- Benton JZ, Williams RJ, Patel A, Meichner K, Tarigo J, et al. Gold nanoparticles enhance radiation sensitization and suppress colony formation in a feline injection site sarcoma cell line, in vitro. *Res Vet Sci.* 2018; 117: 104-110.
- Hainfeld JF, Dilmanian FA, Slatkin DN, & Smilowitz HM. Radiotherapy enhancement with gold nanoparticles. *J Pharm Pharmacol.* 2008; 60: 977-985.
- McMahon SJ, Hyland WB, Muir MF, Coulter JA, Jain S, et al. Biological consequences of nanoscale energy deposition near irradiated heavy atom nanoparticles. *Sci Rep.* 2011; 1: 18.
- Hall EJ, Giaccia AJ. *Radiobiology for the radiologist.* (Wolters Kluwer Health/Lippincott Williams & Wilkins, Philadelphia). 2012.
- Andreev OA, Engelman DM, & Reshetnyak YK. Targeting acidic diseased tissue: New technology based on use of the pH (Low) Insertion Peptide (pHLIP). *Chim Oggi.* 2009; 27: 34-37.
- Dische S, Saunders M, Barrett A, Harvey A, Gibson D, et al. A randomised multicentre trial of CHART versus conventional radiotherapy in head and neck cancer. *Radiother Oncol.* 1997; 44: 123-136.
- Hubbell JH, Seltzer SM (Tables of X-Ray Mass Attenuation Coefficients and Mass Energy-Absorption Coefficients (version 1.4). National Institute of Standards and Technology, Gaithersburg, MD. 2016, January 21 (Original 2004).
- Yao L, Daniels J, Moshnikova A, Kuznetsov S, Ahmed A, et al. pHLIP peptide targets nanogold particles to tumors. *Proc Natl Acad Sci U S A.* 2013; 110: 465-470.
- Rofstad EK, Brustad T. Tumour growth delay following single dose irradiation of human melanoma xenografts. Correlations with tumour growth parameters, vascular structure and cellular radiosensitivity. *Br J Cancer.* 1985; 51: 201-210.
- Robins JM & Rotnitzky A. Semiparametric Efficiency in Multivariate Regression Models with Missing Data. *J Am Stat Assoc.* 1995; 90: 122-129.
- Spiegelhalter DJ, Best NG, Carlin BP, Van der Linde A. Bayesian measures of model complexity and fit (with discussion). *J R Stat Soc Series B Stat Methodol.* 2002; 64: 583-639.
- Cox DR. *Regression Models and Life-Tables.* *J R Stat Soc Series B Stat Methodol.* 1972; 34: 187-220.

34. Kramer CY. Extension of Multiple Range Tests to Group Means with Unequal Numbers of Replications. *Biometrics*. 1956; 12: 307-310.